

Three-dimensional convolution assisted thermal image enhancement for defect detection in composite materials

by F. Wang*, Z. Jiang*, J. Jiang*, Y. Yao** and Y. Liu*

* Institute of Process Equipment and Control Engineering, Zhejiang University of Technology, Hangzhou, 310023 China, 2112102479@zjut.edu.cn, jiangzl@zjut.edu.cn, 221123020532@zjut.edu.cn, yliuzju@zjut.edu.cn

** Department of Chemical Engineering, National Tsing Hua University, Hsinchu, 30013, Taiwan, yyao@mx.nthu.edu.tw

Abstract

Deep learning plays an important role in the field of non-destructive testing of carbon fiber reinforced polymer. A feature extraction method for three-dimensional convolutional autoencoder thermography (3DCAT) is proposed for infrared thermography defect detection, aiming at effectively capturing the potential changes and defect information inside the material. The feature extraction capability of the encoder is enhanced by 3D convolution operation, which realizes the effective processing of infrared thermal imaging data at different time points, resulting in more accurate defect detection. The effectiveness of the proposed method was verified by tests performed on a carbon fiber reinforced polymer containing six defects.

Keywords: non-destructive testing, infrared thermography, 3D convolution, autoencoder

1. Introduction

Non-destructive testing (NDT) [1,2] is a non-destructive method of material evaluation that is widely used in industry as well as in scientific research. Compared with traditional destructive testing methods, NDT technology, using acoustic waves, electromagnetic waves, optics, and thermodynamics [3,4], can provide a comprehensive and accurate assessment of a material's internal structure and properties without affecting its integrity. Among them, infrared thermography (IRT) [5,6], as an NDT method based on the principles of heat conduction and radiation, has attracted much attention in recent years.

IRT can detect and analyse defects, foreign objects or uneven heat distribution within a material using heat distribution images of the object's surface, thus providing a comprehensive and efficient means of evaluating the structure and properties of the material. However, during experiments, thermal images captured by infrared thermography may be affected by a variety of factors, resulting in the appearance of inhomogeneous backgrounds and noise. Some of the common factors include ambient temperature variations, the equipment's own heat, surface reflections, and uneven heat transfer. These factors may interfere with the thermal signal to the region of interest (ROI), reducing the quality and resolution of the image. Therefore, measures to minimize the impact of external factors on thermal images are essential to ensure the reliability of the data.

With the aim of solving the above-mentioned problems in the acquired thermal images, researchers have adopted various methods to improve the quality and accuracy of the images [7,8]. Among them, thermal signal reconstruction [9] helps to remove background noise and inhomogeneity and improve image resolution and contrast-to-noise ratio. However, there are still a high number of images with improved quality, and observations by researchers are still time-consuming and labour-intensive. Thus, reducing the number of thermal images and pooling multiple defects onto a small number of thermal images has become the research goal of many researchers. Principal Component Thermography (PCT) [10], a widely recognized feature extraction method, significantly reduces the number of images by extracting the main feature components of thermal image data. Nevertheless, since thermal image data are more nonlinear, researchers have successively proposed a variety of nonlinear machine learning methods [10] and achieved significant results in practice.

In recent years, deep learning [11,12], as a branch of machine learning, has attracted extensive attention and research. Its applications in computer vision, natural language processing and other fields [13,14] have achieved many breakthroughs. Deep learning has demonstrated superior performance in processing IRT data compared to traditional machine learning methods. Autoencoder (AE), as a neural network model for unsupervised learning, has been successfully applied in many fields such as image processing, speech recognition, and anomaly detection [15,16], and has demonstrated excellent performance and potential. In the field of IRT, AE is widely used in feature extraction [17] and data enhancement [18] to solve different difficulties encountered in IRT. However, due to the process of acquiring thermal images, there is more obvious time series information in the acquired thermal image data. Although the traditional two-dimensional (2D) convolution has achieved remarkable results in the field of image processing, it has some limitations in processing three-dimensional (3D) data [19].

With the development and popularization of 3D convolution, it has been possible to better utilize the spatial information of the data to achieve effective modelling and analysis of 3D data. 3D Convolutional Neural Networks can capture both temporal and spatial features in the data while enabling feature extraction in all three dimensions. To explore



the potential of 3D convolution in the field of IRT, a feature extraction method for 3D Convolutional Autoencoder Thermography (3DCAT) is proposed. Utilizing the dual advantages of 3D convolution and AE, it is possible to synthesize the temporal and spatial information in thermal image data to effectively capture potential changes and defect information at different time points. Subsequently, conventional PCT was utilized to further reduce the number of thermal images and allow defects to be more clearly displayed into a smaller number of thermal images. Finally, 3DCAT was applied to a carbon fibre reinforced polymer (CFRP) sample with six defects for testing and compared with other methods to validate the effectiveness of the proposed method.

2. Data Acquisition and Preprocessing

The thermal imaging data used during the experiments can be acquired by the IRT device. In this study, the specific equipment mainly consists of CFRP samples to be tested, two flash lamps, infrared camera and computer, the detailed visit is shown in Figure 1. A heat pulse is radiated onto the sample to be tested after it has been briefly heated by a flash lamp. Subsequently, an infrared camera was used to record changes in the surface temperature of the sample during the cooling process. When there is a defect inside the sample, the different physical properties of the sample and the defect, such as material density, specific heat capacity, thermal conductivity, etc., lead to the creation of different temperature attenuation regions. This temperature contrast can be observed and recorded by an infrared camera. Next, in the acquired infrared thermograms, a clear difference will be observed by direct observation. The acquired n_t images of size $n_x \times n_y$ are processed through a computer. The final 3D matrix of $n_t \times n_x \times n_y$ can be obtained for subsequent experimental testing. In further experiments, to optimize the model performance and improve the convergence speed of the algorithm, a Min-Max normalization strategy is adopted to process the data. The 3D matrix is transformed into a 2D matrix $n_t \times n_x n_y$, where each row represents a thermal image, and each column represents the temperature change of the same pixel. Min-Max normalization was used to preprocess each row of the 2D matrix to ensure that each pixel value in the data was constrained to the range [0, 1].

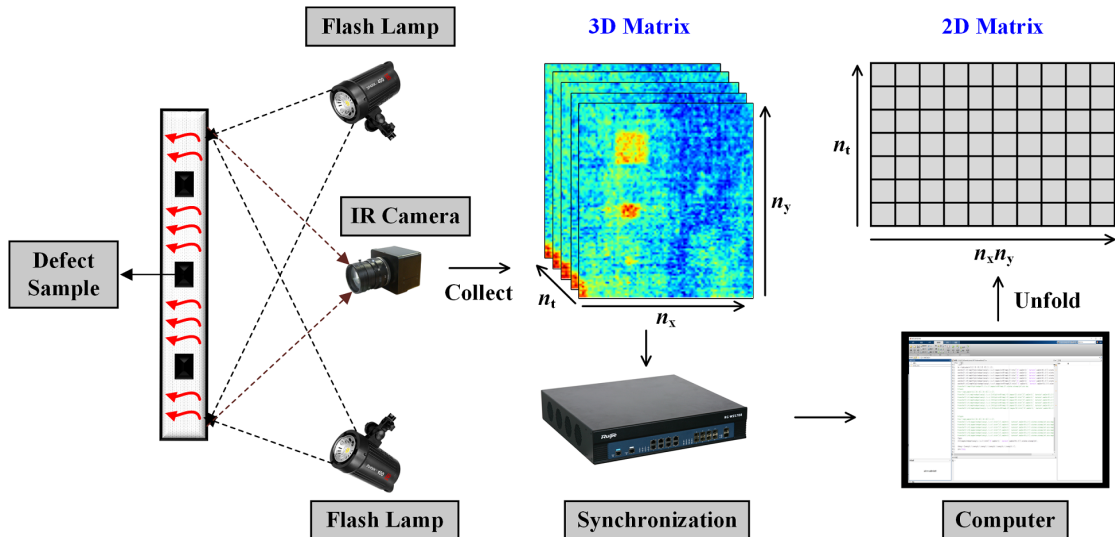


Fig. 1. Distribution of IRT experiments

3. Methodology

3.1. The Basic of 3D Convolutional AE

In 2D convolution, a small convolution kernel is utilized to slide over the input image. It operates by convolving with each position of the input image and is mainly used to extract features in a single thermal image. By training the neural network, the weights of these convolution kernel can be learned to capture different features in the input image. Multiple convolution kernel can be applied in parallel to the input image to extract different features. Usually, the number of channels is equal to the number of convolution kernel used. However, 3D convolution is a convolution operation performed on 3D data. Like 2D convolution, 3D convolution uses convolution kernels to perform convolution operations at each location of the input data to extract features. The difference is that the 3D convolution operation considers three dimensions of the thermal image data. In 3D convolution, the convolution kernel is a 3D tensor. It slides along all dimensions of the input data and performs convolution operations with the local cubic regions of the data. In thermal image data, the number of images can be significantly reduced by 3D convolution, which can be reflected in thermal image data.

Like traditional AE, 3D Convolutional AE (3DCAE) also consists of two parts: an encoder and a decoder. The encoder progressively compresses the input data into a latent representation by means of multiple 3D convolutional layers,

where the feature maps of each layer are processed by a nonlinear activation function. The decoder, on the other hand, maps the encoded latent representations back to the original 3D data space through a 3D deconvolutional layer. The output of the encoder is a feature map, which represents a characteristic representation of the data at different levels. If $\mathbf{X} \in \mathbf{R}^{M \times N \times T}$ denotes a set of infrared thermal imaging data, then M , N and T denote its length, width, and number of sheets, respectively. The process of extracting features and reconstruction of infrared thermal imaging data using 3DCAE is denoted as:

$$\mathbf{X}_{\text{mid}} = f(\mathbf{W}_{\text{en}} \cdot \mathbf{X}_{\text{en}} + \mathbf{b}_{\text{en}}) \quad (1)$$

$$\mathbf{X}_{\text{de}} = g(\mathbf{W}_{\text{de}} \cdot \mathbf{X}_{\text{mid}} + \mathbf{b}_{\text{de}}) \quad (2)$$

where $\mathbf{X}_{\text{mid}} \in \mathbf{R}^{M \times N \times t}$ ($t \ll T$) denotes the features extracted by the encoder and t is the number of tensors of the feature map; $\mathbf{X}_{\text{de}} \in \mathbf{R}^{M \times N \times T}$ denotes the infrared thermal imaging data reconstructed by the decoder; \mathbf{W}_{en} and \mathbf{W}_{de} represent the weight values of the encoder and decoder, respectively; and \mathbf{b}_{en} and \mathbf{b}_{de} represent the biases of the encoder and decoder. When weights and biases are continuously trained through neural networks, they look for patterns and features in the input data. By gradually adjusting the weights and biases, the network attempts to minimize the difference between the input data and its own reconstruction. This process typically results in 3DCAE learning effective representations of the data, i.e., features. They can represent the input data efficiently in a lower dimensional space.

When a set of 3D thermal image data is input to 3DCAE, this data will be continuously trained through the model to the encoder and decoder. The encoder compresses the width, height, and number of thermal image data to lower dimensions through 3D convolution to achieve feature extraction in each of the three dimensions. Then the decoder can remap the features of the low-dimensional space obtained by the encoder back to the original data space, thus realizing the reconstruction of the data. In this paper, the middle layer (i.e., encoder results) is extracted to achieve 3D feature extraction from the data. This study will focus more on utilizing the encoder results as a pre-detection map for defect detection for subsequent processing.

3.2. 3DCAT Model Construction and Training

To validate the effectiveness of 3DCAE on thermal image data. After several tests, this paper constructs 3D convolutional autoencoder thermography (3DCAT) where the encoder consists of three 3D convolutional blocks and the decoder consists of three 3D anti-convolutional blocks. In the encoder, the first convolutional layer uses a $4 \times 4 \times 4$ convolutional kernel, a stride size of $2 \times 2 \times 2$, and a padding of 1. The second and third convolutional kernels, on the other hand, use a $4 \times 3 \times 3$ convolutional kernel, a stride size of $2 \times 1 \times 1$, and a padding of 1. The decoder, on the other hand, is like the encoder, using the same convolution kernel, step size and padding in the corresponding deconvolution block. However, it is worth noting that the LeakyReLU activation function with a negative slope of 0.02 is used for the remaining layers including the encoder, except in the last layer of the decoder where the Tanh activation function is used. The specific model structure is shown in Figure 2. The spatial and temporal dimensionality reduction of thermal image data is realized by the subtle stride design of the 3DCAT model. It not only retains the main features of the input data, but also reduces the three dimensions of the thermal image data, which in turn enables efficient dimensionality reduction of the data.

To maximize the model performance as much as possible and to speed up the convergence of the algorithm, Min-Max normalization is applied to each row of the acquired thermal image data. Doing so not only significantly improves the quality of the data, but also provides a better fit to the inputs of subsequent models in preparation for model training. Subsequently, the thermal image data was adjusted to a size suitable for network input as input data to the model. The model that receives the input data utilizes the encoder and decoder for its feature extraction and data reconstruction. In this training process, the choice of parameters is crucial for the performance of the model and the speed of convergence. After several tests, a learning rate of 0.002, a training batch of 100, and a batch size of 1 are set. The mean square error is chosen as the loss function of the model and Adam is chosen as the optimizer for training. And the model parameters are updated using the back propagation algorithm. After reaching a preset number of training batches, the results of the completed encoder are used as the training results of the model, i.e., 3D feature extraction is realized on the original data. Since the output of the encoder is a multi-channel result, it is processed here by summing and averaging the results of multiple channels. Subsequently, this result is used for subsequent comparison experiments for further in-depth discussion.

3.3. Further Dimensionality Reduction

After the encoder extraction of 3DCAT, the feature maps obtained after feature extraction can characterize a large amount of defect information, but still have many thermal image maps, which are still time-consuming and laborious to manually detect sequentially. Therefore, the selection of subsequent data processing methods is crucial. PCT, the most widely applicable dimensionality reduction technique in the field of IRT, is used to discover key features and patterns in thermal image data. The basic idea is to map high-dimensional data into a low-dimensional space while trying to preserve

the original information of the data. Dimensionality reduction of data is achieved by calculating the covariance matrix of the data, finding the main directions of variance in the data, and projecting the data onto these directions. In PCT, these principal directions of variance are called principal components (PCs), which are linear combinations in the data. By retaining the most important principal components, dimensionality reduction of the data can be achieved while still retaining most of the key information of the original data. Subsequently, the number of principal components needed is set to k ($k < t$) (i.e., k PC images will eventually be obtained). The resulting 2D matrix $k \times n_x n_y$ is finally visualized. It can be found that all k thermal image maps contain most of the information of the thermal image data.

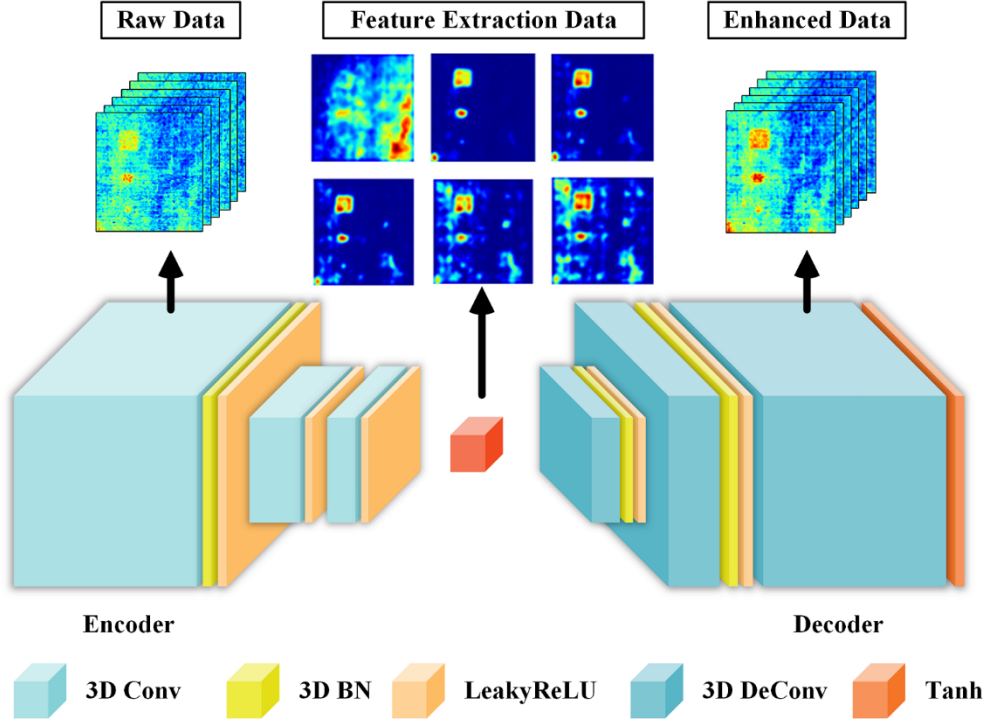


Fig. 2. 3DCAT modelling framework

4. Experiment

To verify the validity of the 3DCAT model, tests were performed on a CFRP specimen containing six internal defects. It is also compared with the traditional PCT method and 2DCAT method to demonstrate the performance that the methods have in defect detection. To further demonstrate the effectiveness of the proposed method, the contrast-to-noise ratio (CNR) metric [20] was used to objectively evaluate the performance. CNR is a measure used in various fields (including imaging and signal processing) to quantify the quality of an image or signal [21, 22]. It will evaluate the relative differences in signal strength and the variability of background noise in the ROI. The specific CNR formula can be expressed as:

$$\text{CNR} = \frac{|A_{\text{def}} - A_{\text{non}}|}{S_{\text{non}}} \quad (3)$$

where A_{def} and A_{non} denote the average pixel values of the defective and non-defective regions in the thermal image, respectively, and S_{non} denotes the standard deviation of the pixel values of the non-defective regions. CNR measures the contrast between defective and non-defective areas. A high CNR value usually implies that the method is more capable of recognizing defects. In image processing, an increase in the CNR value means that defects are more clearly distinguished from background noise. This clear contrast helps to improve the reliability and accuracy of defect detection.

4.1. CFRP Sample Production and Data Collection

The CFRP specimens used in this study were fabricated using a resin transfer moulding apparatus. Three different sizes of Teflon inserts were placed in the carbon fiber layer to simulate defects. The locations of the six defects are shown in Figure 3. The shape, size and depth of each defect are detailed in Table 1. The CFRP specimens were heated instantaneously using two flash lamps. During the cooling phase, an infrared camera was used to collect surface

temperature data of the samples at different sampling moments to obtain thermal images of the CFRP. Subsequently, 59 thermal images were obtained after eliminating corrupted data. Each thermal image was cropped to a thermal image with an ROI size of 90×100. The final infrared thermal imaging dataset obtained is 59×90×100 in size. For subsequent analysis, the dataset was expanded into a 59×9000 2D matrix, each row of which corresponds to a thermal image, and each column represents the temporal variation of a pixel value.

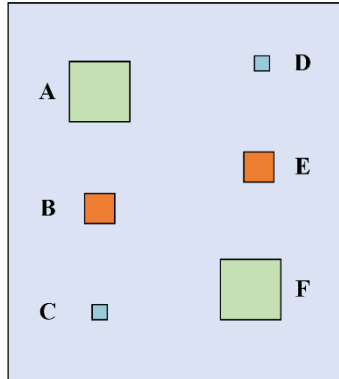


Fig. 3. Schematic diagram of defect distribution

Table 1. Defect information of CFRP specimens

Number	Shape	Area(mm ²)	Depth(mm)
A	Square	16 × 16	2.6
B		8 × 8	
C		4 × 4	
D		4 × 4	5.2
E		8 × 8	

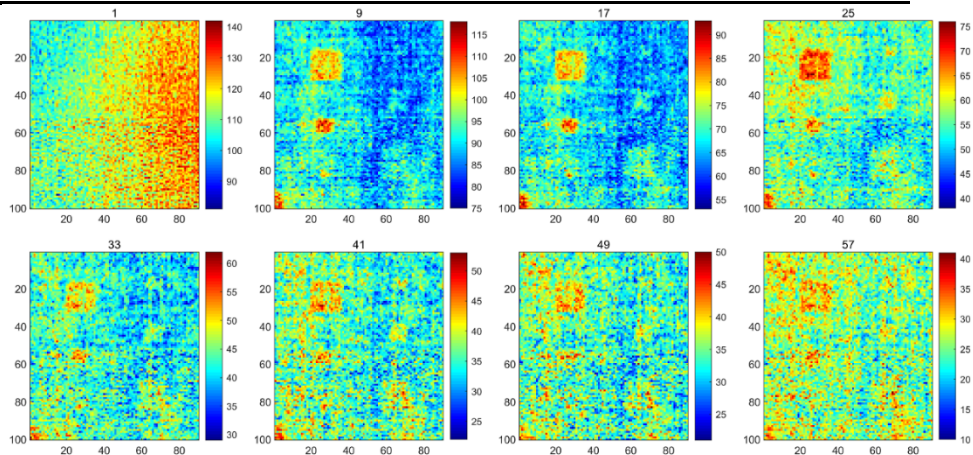


Fig. 4. Thermal images sampled at eight different moments

Figure 4 shows the thermal image data at eight different sampling moments. It can be noticed from the thermal image that inhomogeneous background and noise seriously affect the observation of defects. Therefore, it is particularly important to develop thermographic data analysis methods to reduce the interference of inhomogeneous background and noise.

4.2. 3DCAT Training and Comparison

After normalizing the above acquired thermal image data by rows, it was adapted to a 64×128×128 matrix to facilitate the input to the model for training. And the adjusted matrix data is fed into the 3DCAT model for training. At the end of training according to the set batch, the encoder result is extracted as a pre-detection maps. The encoder results for 3DCAT are shown in Figure 5. It can be observed that a large amount of inhomogeneous background and noise have been removed. Most of the six defects buried in the CFRP are presented in the thermal image, with the three shallower defects on the left side being more visible.

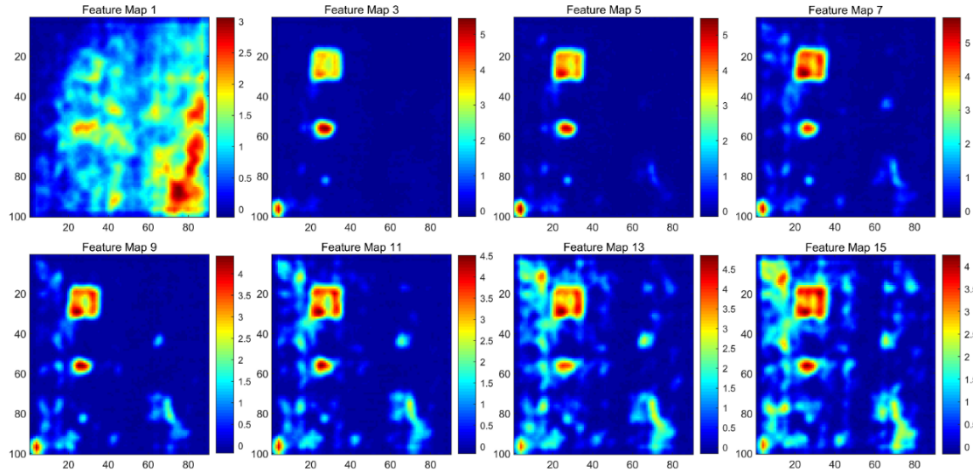


Fig. 5. 3DCAT encoder feature maps

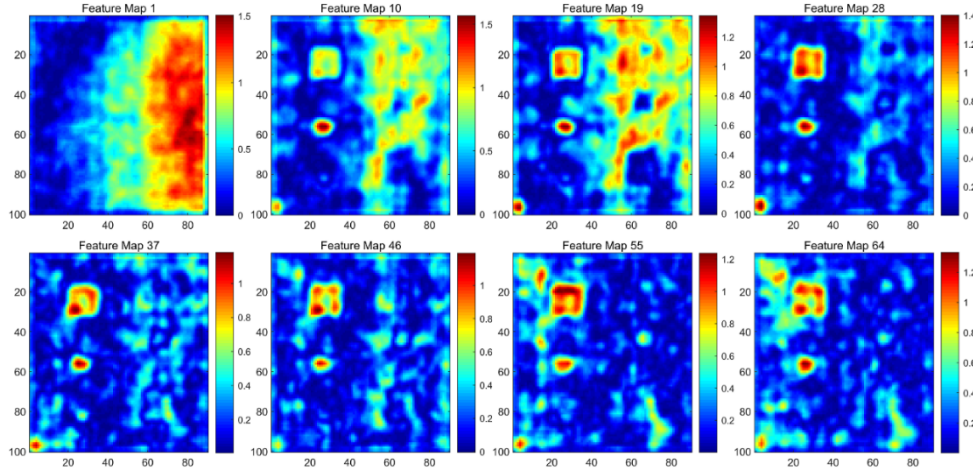


Fig. 6. 2DCAT encoder feature maps

Modify the 3D convolution in the 3DCAT model to 2D convolution and set similar network structure and parameters. The thermal image data was processed in the same preprocessing manner and then input into the 2DCAT model for training. This was done to validate the effectiveness of the 3DCAT model for feature extraction in the time dimension. When extracting the encoder results, it can be noticed that 3DCAT can achieve dimensionality reduction in the time dimension, thus reducing the number of thermal images. The encoding result of 3DCAT will present a large amount of information to a smaller number of thermal images. And the number of encoder feature maps for 2DCAT was not reduced, which means it did not achieve feature extraction in the time dimension. As shown in Figure 6, eight encoder results of 2DCAT are selected for visualization.

4.3. 3DCAT Training and Comparison

By extracting the 3DCAT encoder results, although the number of thermal images has been reduced, there is still the problem of not being able to detect them efficiently. To achieve fair comparisons, further data dimensionality reduction is achieved for them using traditional PCT. To verify the validity of the method, its further dimensionality reduction results are compared with the PCT results of the original data and the PCT results of the 2DCAT encoder at the same time.

The PCT defect detection results of the raw data are shown in Figure 7(a). Three defects in the shallow left side can be observed in PC1 under the influence of a large amount of noise. But in all other images are filled with a lot of noise. The visualized image after PCT processing of 2DCAT encoder is shown in Figure 7(b). Observation reveals that a large amount of noise has been removed and the three defects on the left are more clearly shown in the image. However, the deeper defects on the right side are affected by the inhomogeneous background and should not be observed. The visualization of the model encoder results in this paper after PCT processing is shown in Figure 7(c). It can be noticed in PC1 that the original inhomogeneous background and noise have been removed. All six defects inserted in the sample were detected. The larger of these defects show a different colour from the background displayed in the thermal image. In PC2, the defects in the samples are similarly characterized. The effectiveness of the method proposed in this paper can be seen through the thermal images.

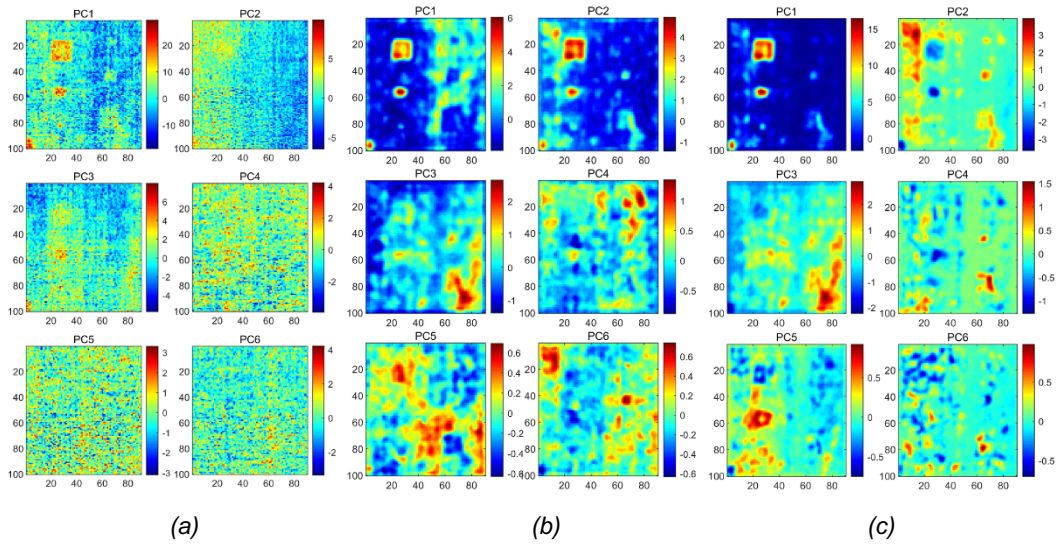


Fig. 7. PCT results for several different data types for CFRP specimens: (a) Original; (b) 2DCAT; (c) 3DCAT.

Comparing the three sets of results reveals that the effect of noise on defect detection can be significantly attenuated by convolutional operations. Further observation reveals that a large amount of inhomogeneous background is removed after dimensionality reduction of the time dimension is achieved by 3D convolution. This phenomenon is particularly evident in PC1 in Figure 7(c). When the data is entered into the 3DCAT model, it will be processed in both the spatial and temporal dimensions. In short, in feature extraction and reconstruction of the thermographic data, the model considers not only its spatial information, but also the variation of its temporal information. This approach will allow the model to capture dynamic changes and deep features more effectively in thermal image data. Therefore, compared to the 2DCAT model, the 3DCAT model can mine the information of the data more fully, thus improving the performance level of the model.

Table 2. CNR values after PCT for each model

Method	Defect A	Defect B	Defect C	Defect D	Defect E	Defect F
Original	2.15	2.23	1.49	1.04	1.39	1.34
2DCAT	5.36	4.95	1.22	1.31	2.28	2.51
3DCAT	5.63	5.06	1.85	1.54	3.52	3.47

To further enhance the credibility of the model results, CNR was utilized to evaluate its performance. As shown in Table 2, the CNR values of the PCT results for the three different data are presented. The comparison reveals that the proposed 3DCAT model exhibits higher CNR values. This also reflects the superior performance of the model in defect detection. This finding emphasizes the importance of the ability of 3D convolution to consider both temporal and spatial information compared to 2D convolution. Further, the 3DCAT model considers thermal imaging data from before and after time, providing the model with more robust feature extraction capabilities. It makes it particularly effective in further utilizing PCT dimensionality reduction.

5. Conclusion

In this study, 3D convolution technique is introduced into the IRT field, and a 3DCAT-based feature extraction method for thermography is proposed. Compared to traditional 2D convolution methods, 3D convolution can capture spatial and temporal information in thermal imaging data more comprehensively. By extracting the encoder results, feature extraction of spatial and temporal information of thermographic data can be effectively realized. After training, the model encoder will be able to effectively characterize the feature information of thermal imaging data. To further validate the effectiveness of the method, a CFRP sample with six defects was selected for experimental testing. The raw data as well as the 2DCAT and 3DCAT encoder results were dimensionality reduced using PCT and then analysed in a comprehensive comparison. Future research directions can consider applying 3D technology in generating adversarial networks to solve

the problem of insufficient diversity of thermal image data and further promote the development of thermal imaging technology.

ACKNOWLEDGMENTS

The authors gratefully acknowledge the National Natural Science Foundation of China (Grant No. U23A20328) and the Fundamental Research Funds for the Provincial Universities of Zhejiang (No. RF-C2022002) for financial support. Yao was supported in part by the National Science and Technology Council, ROC under project number NSTC 112-2221-E-007-105.

REFERENCES

- [1] Silva M I, Malitckii E, Santos T G, et al. Review of conventional and advanced non-destructive testing techniques for detection and characterization of small-scale defects. *Progress in Materials Science*, 2023: 101155.
- [2] Ramírez I S, Márquez F P G, Papaelias M. Review on additive manufacturing and non-destructive testing. *Journal of Manufacturing Systems*, 2023, 66: 260286.
- [3] Tuschl C, Oswald-Tranta B, Agathocleous T, et al. Scanning inductive pulse phase thermography with changing scanning speed for non-destructive testing. *Quantitative InfraRed Thermography Journal*, 2023: 1–16.
- [4] Jodhani J, Handa A, Gautam A, et al. Ultrasonic non-destructive evaluation of composites: A review. *Materials Today: Proceedings*, 2023, 78: 627–632.
- [5] Vavilov V P, Bison P G, Burleigh D D. Ermanno Grinzato's contribution to infrared diagnostics and nondestructive testing: in memory of an outstanding researcher. *Quantitative InfraRed Thermography Journal*, 2023: 1–14.
- [6] Helvig K, Trouvé-Peloux P, Gaverina L, et al. Automated crack detection on metallic materials with flying-spot thermography using deep learning and progressive training. *Quantitative InfraRed Thermography Journal*, 2023: 1–20.
- [7] Liu, KX.; Ma, ZY.; Liu, Y.; Yang, JG.; Yao, Y. Enhanced defect detection in carbon fiber reinforced polymer composites via generative kernel principal component thermography. *Polymer*, 2021, 13.
- [8] Liu, Y.; Liu, KX.; Gao, ZL.; Yao, Y.; Sfarra, S.; Zhang, H.; Maldague, XPV. Non-destructive defect evaluation of polymer composites via thermographic data analysis: A manifold learning method. *Infrared physics & technology*, 2019, 97.
- [9] Shepard, SM.; Lhota, JR.; Rubadoux, BA.; Wang, D.; Ahmed, T. Reconstruction and enhancement of active thermographic image sequences. *Optical engineering*, 2003, 42, 1337–1342.
- [10] Rajic, N. Principal component thermography for flaw contrast enhancement and flaw depth characterisation in composite structures. *Composite structures*, 2002, 58, 521–528.
- [11] Garrido I, Lagüela S, Fang Q, et al. Introduction of the combination of thermal fundamentals and Deep Learning for the automatic thermographic inspection of thermal bridges and water-related problems in infrastructures. *Quantitative InfraRed Thermography Journal*, 2023, 20(5): 231–255.
- [12] Mohammed A, Kora R. A comprehensive review on ensemble deep learning: Opportunities and challenges. *Journal of King Saud University-Computer and Information Sciences*, 2023, 35(2): 757–774.
- [13] Ma D, Dang B, Li S, et al. Implementation of computer vision technology based on artificial intelligence for medical image analysis. *International Journal of Computer Science and Information Technology*, 2023, 1(1): 69–76.
- [14] Bharadiya J. A comprehensive survey of deep learning techniques natural language processing. *European Journal of Technology*, 2023, 7(1): 58–66.
- [15] Liu Y, Wang F, Liu K, et al. Deep convolutional autoencoder thermography for artwork defect detection. *Quantitative InfraRed Thermography Journal*, 2023: 1–17.
- [16] Masaki A, Nagumo K, Oiwa K, et al. Feature analysis for drowsiness detection based on facial skin temperature using variational autoencoder: a preliminary study. *Quantitative InfraRed Thermography Journal*, 2023, 20(5): 304–318.
- [17] Liu, KX.; Zheng, MK.; Liu, Y.; Yang, JG.; Yao, Y. Deep autoencoder thermography for defect detection of carbon fiber composites. *IEEE transactions on industrial informatics*, 2023, 19, 6429–6438.
- [18] Li, XY.; Ying, XW.; Zhu, W.; Liu, W.; Hou, BP.; Zhou, L. Nondestructive detection and analysis based on data enhanced thermography. *Measurement science and technology*, 2022, 33.
- [19] Maken P, Gupta A. 2D-to-3D: a review for computational 3D image reconstruction from X-ray images. *Archives of Computational Methods in Engineering*, 2023, 30(1): 85–114.
- [20] Ibarra-Castanedo, C.; Piau, JM.; Guilbert, S.; Avdelidis, NP.; Genest, M.; Bendada, A.; Maldague, XPV. Comparative study of active thermography techniques for the Nondestructive evaluation of honeycomb structures. *Research in nondestructive evaluation*, 2009, 20, 1–31.
- [21] Bu C.; Li R.; Liu T.; et al. Micro-crack defects detection of semiconductor Si-wafers based on Barker code laser infrared thermography. *Infrared Physics & Technology*, 2022, 123: 104160.
- [22] Ebrahimi S, Fleuret J, Klein M, et al. Robust principal component thermography for defect detection in composites. *Sensors*, 2021, 21(8): 2682.